INFLUENCE OF DOPANT CONCENTRATION ON THE STRUCTURAL AND OPTICAL PROPERTIES OF NANOCRYSTALLINE ZnS:In FILMS

TULAY HURMA *

Department of Physics, Eskisehir Technical University, TR-26470, Eskişehir, Turkey

ZnS and ZnS:In films containing three different rates of In were produced on glass subtrates heated up to 300±5°C. Structural analyses of the films were done by X-ray diffraction (XRD), Raman and Infrared (FT-IR) spectroscopies. It was determined that the films obtained by ultrasonic spray pyrolysis (USP) method had polycrystalline structure. All observed XRD peaks belong to hexagonal wurtzite ZnS structure. Crystallite sizes of the films were approximately calculated in 4.61-4.63 nm range. SEM images showed that particles have homogeneously distributed and held onto surface. It was observed from the EDS results that the In rate of films increased by increasing In doping in the solution. FTIR spectra revealed presence of four significant peaks. Peak observed around 930 cm^{-1} corresponded to the Zn-S vibration while, smaller peaks around 3500 cm^{-1} corresponded to the –OH group of H_2O stretching. The aromatic ring C–H bending vibrations gave the peaks around 750 cm^{-1}. The optical properties of ZnS and ZnS: In films were investigated by optical transmittance and reflectance spectra.

Keywords: *In doped ZnS film; XRD; Raman; Optical properties*

1. Introduction

Nowadays, nanostructured organic structures and thin films are sources of great hopes and leading to nanotechnology. CdS and ZnS nanostructures as the most important representatives of II-VI group semiconductors, are frequently used in the field of optoelectronics. These semiconductors with wide optical band gap have created new opportunities for the development of optical work and applications [1-4]. The electronic, linear and nonlinear optical characteristics of these materials make it possible to use them in the production of various devices. The development of solar cells and production of optical circuit elements such as optical memories, optical transistors and LEDs can be given as examples to their practices in the field of optoelectronics [5]. The technologies that use solar energy have been gradually getting more efficient and accessible through developing technologies. CdS is the most promising buffer layer for thin-film heterojunction solar cells and the highest conversion efficiency of Cu (In, Ga) Se_2 solar cells have been obtained with CdS buffer layer [6-8]. However, the produced CdS causes serious environmental problems due to its wastes arising during and after production phase which contain highly toxic cadmium content. In addition to this, band gap of CdS is 2.42 eV [9] and this corresponds to a wavelength around 520 nm. Therefore, the light with a wavelength lower than 520 nm cannot be transmitted to the light absorbing layer and this decreases quantum efficiency at short wavelength zone [10]. Therefore, developing a buffer layer without Cd is one of the main objectives of solar cell production. ZnS is more environment-friendly compared to CdS. ZnS acts transparent to almost all wavelengths of solar spectrum at optical band gap at 3.40-3.74 eV and absorbs high-energy photons and increases light absorption of absorbing layer. Furthremore it provides better lattice matching with absorbers having energy band gaps in the range of 1.3–1.5 eV [11- 13]. Therefore, ZnS films have been produced and analyzed in recent years by using different techniques and substrate temperatures [7, 8, 12, 14–21].

As a host material, ZnS is an appropriate semiconductor for dopants used for improving structural and optical characteristics [22]. A semiconductor film with desired properties can be obtained by doping process. The first study on this subject was reported in 1994 by Bhargava and Gallagher [23]. After this date, the doped ZnS films produced by using Al, Cu, Fe, Co dopants were analyzed [24-29]. Apart from these dopants, Abdelhak Jrad et al., analyzed In doped ZnS films by CBD method for the first time [30]. The obtained results confirmed that the doped nanocrystalline films exhibit different interesting properties compared to bulk materials such as increased energy band due to quantum restriction.

In the literature,a few In doped films were produced through various methods. Therefore, in

* Autor corespondent/*Corresponding author*,
E-mail: tulayhurma@gmail.com

this study, nanostructure ZnS:In films containing three different rates of In were produced by using Ultrasonic Spray Pyrolysis (USP) method and the effects of In doping and rate on structural and optical properties of ZnS films were studied. USP technique is preferred for its advantages that it has a simplicity structure, it does not need any vacuum environment and it is an affordable method. The USP technique has several parameters that affect the physical properties of films. These parameters are substrate temperature, spraying rate and time, distance between the substrate and spray-head-atomizer, total amount of sprayed solution and carrier gas.

2. Experimental details

A schematic representation of the USP system used in this study is given in Fig.1. In principle, USP system contains a ultrasonic spray nozzle, a heater for heating the substrate, thermocouple included temperature controller and an air compressor. In this study, solutions containing Zn, S and In were prepared for obtaining ZnS semiconductor films by USP method. Solution of 0.05 M ZnCl2 was used as the Zn source, solution of 0.05M (NH2)CSNH2 as the S source and solution of 0.05M InCl3 as the In source. Solutions to be sprayed for each film were prepared by mixing them in doses given in Table 1. 150 ml solution was sprayed on glass substrates preheated up to 300±5°C at 5 cc/min flowrate. Distance between the nozzle and the substrate was kept fixed at 35 cm, spraying continued for 30 minutes and gas at 1 bar pressure was used as the carrier gas.

Table 1

Precursor solutions of the ZnS and ZnS:In films

Film (ml)	$ZnCl_2$ (ml)	InCl (ml)	H_2NCSNH_2
ZnS	75.00	---	75.00
ZnS:In (1%)	74.25	1.50	74.25
ZnS:In (3%)	72,75	4.50	72.75
ZnS:In (5%)	71.25	7.50	71.25

X-ray diffraction (XRD), Raman and FTIR spectroscopy measurements were used for determining phases of obtained films. XRD measurements were done for determining crystal forms and crystallization sizes of the films. These measurements were done by using BRUKER D8 Advance X-ray diffractometer measurements with CuKα ray at λ=1,541 Å wavelength. Vibrational properties of the films were determined by means of ATR (4 cm-1 resolution) using Perkin Elmer 2000 FT-IR spectrometer and Bruker Senterra Dispersive Raman system (by He_Ne laser). The optical band gaps, refraction indexes, extinction coefficients and

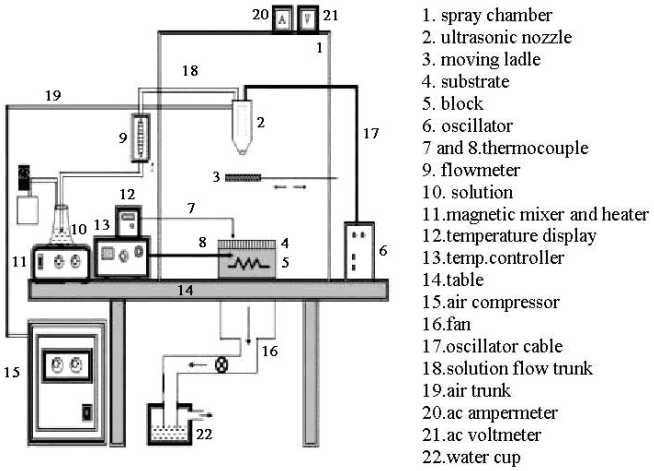

Fig. 1 - Schematic diagram of the ultrasonic spray pyrolysis setup.

optical conductivities of the films were calculated by using transmittance and reflectance spectra taken at 300-900 nm wavelength by using a Shimadzu 2450 UV model spectrophotometer. Surface images of the films were taken by using a field emission scanning electron microscopy (SEM) (ZEISS Ultraplus). Films are produced by spray pyrolysis method with the parameters of the experiment being kept constant, so the thicknesses of the films are very close to each other and are in the order of 300 nm.

3. Results and discussion

3.1 X-ray diffraction analysis and SEM images of the films

In this study, it was determined that the ZnS and ZnS:In films obtained by USP method have polycrystalline structure upon analyzing their XRD patterns (Figure 2). All observed peaks belong to hexagonal wurtzite ZnS structure (JCPDS: 79-2204). With the effect of indium doping, a little decrease was observed in peak intensity of (111) plane and peaks of (002) and (100) planes became distinct. In the ZnS:In 5% film where In rate was maximum, crystallization level towards (111) direction decreased. When indium, a third group element is doped in ZnS, In3+ atoms substitute Zn+2 atoms and act as donors. Generally, at higher doping concentrations, the density of nucleation centers is high, which eventually introduces certain intrinsic stress in the film and disturbs the host (ZnS) lattice. Therefore, the developed micro-strain restricts the growth of crystallites [31]. It has been observed in previous studies that ZnS film has a reduced crystallinity when doped with high In concentrations [31, 32]. One of the III. group elements is Al (aluminum). In previous work, the structural properties of Al-doped ZnS films were investigated and found to lower the crystallinity of higher Al doping [33]. Crystallite sizes of the films were calculated around 4.61-4.63 nm range by

means of the well-known Scherrer formula. In doping did not significantly change the crystal size. In the previous work, Al was doped into the ZnS films and a decrease in crystal size was observed [33].

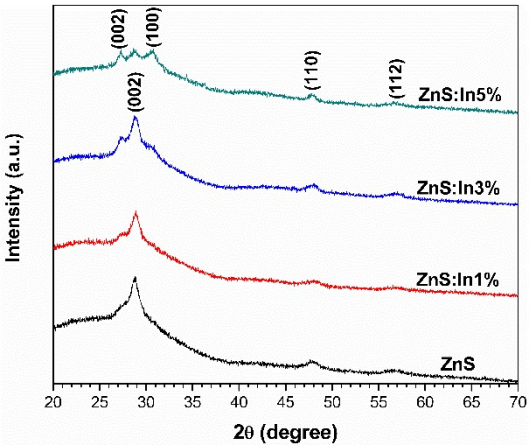

Fig. 2 - XRD spectra of the nanostructured ZnS and ZnS:In films.

Surface images of the films were analyzed by SEM images and they are shown in Figure 3. As a result of SEM analyses, it was confirmed that the films have nm size particles. In addition, SEM images showed that the films were coated homogenously on the surface. As solution droplets do not completely evaporate by coming closer to the substrate, accumulated formations with extra large particles were observed over the smooth background of the ZnS:In 1% film. Furthermore, film surfaces became rougher by increasing In rate. The corresponding EDS spectra as shown in Figure 4 confirm the presence of all expected elements including Zn, S and In. It is seen from the EDS results that the In rate of films increases by increasing In rate of precursor solutions.

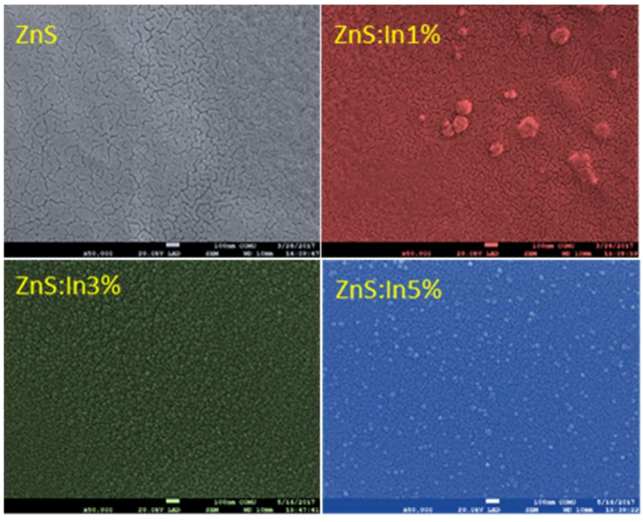

Fig. 3 - SEM images of the nanostructured ZnS and ZnS:In films.

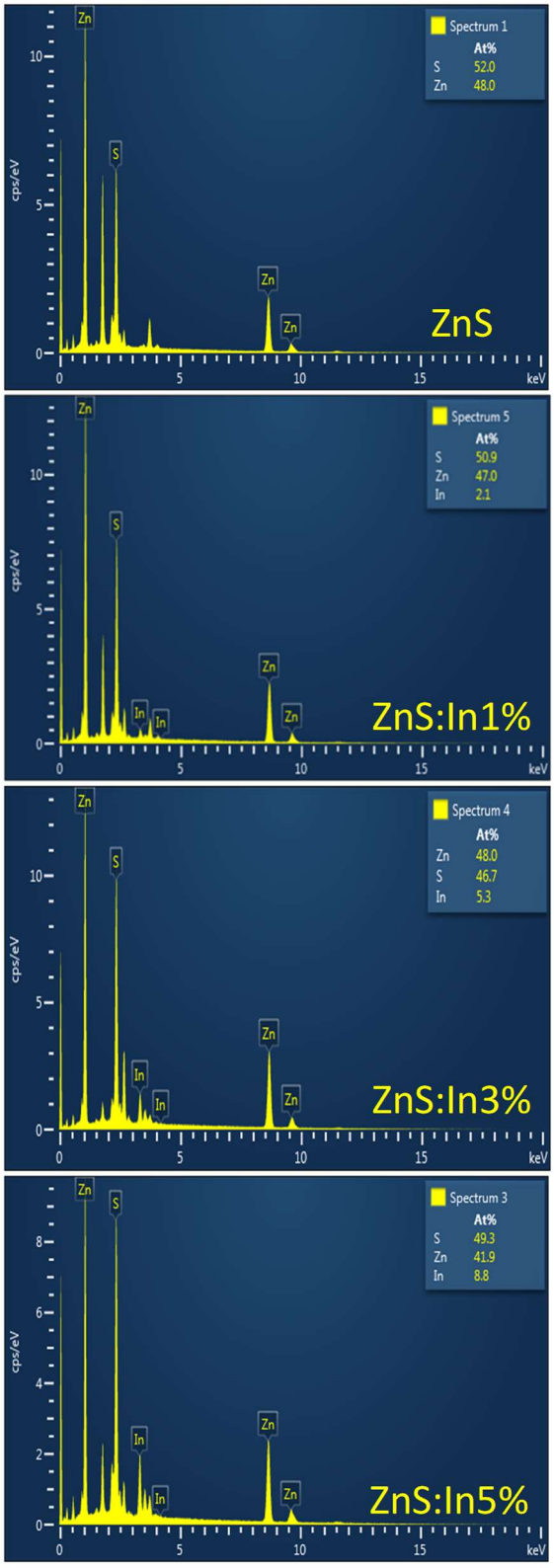

Fig. 4 - EDS spectra of the nanostructured ZnS and ZnS:In films.

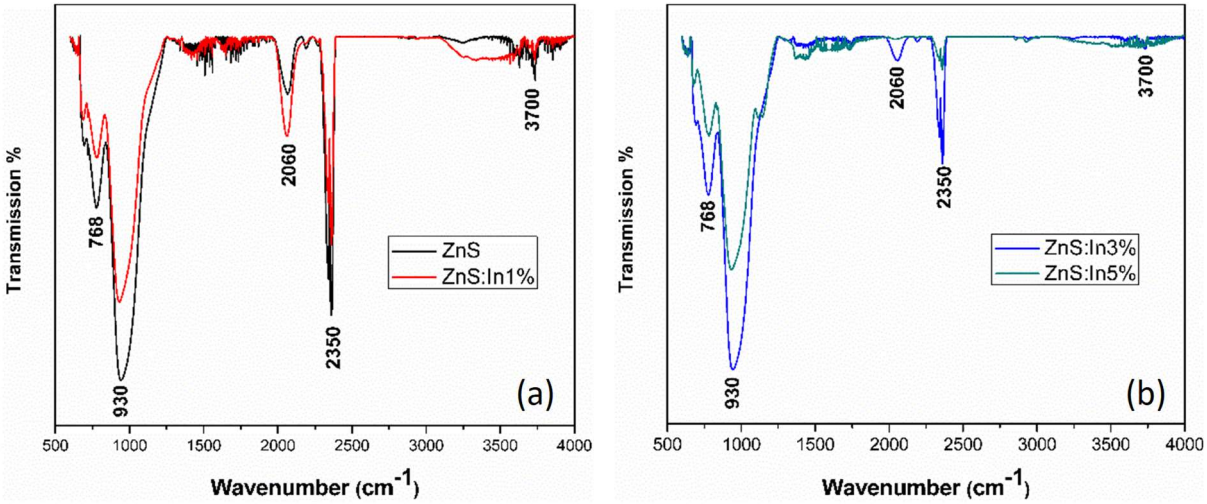

Fig. 5 - FTIR spectra of the nanostructured ZnS and ZnS:In films.

3.2. FTIR and Raman spectroscopy of the films

FTIR study can identify the types of functional groups on the surfaces and might enable us to recognize molecular foreign matters. In this study FTIR spectra of produced undoped and In doped ZnS films are shown in Figure 5. FTIR spectra have presented presence of four significant peaks. Peak observed around 930 cm^{-1} corresponded to the Zn-S vibration while, smaller peaks around 3500 cm^{-1} corresponded to the OH group of H2O stretching [34]. The peak observed around 2060 cm^{-1} corresponded to the C-H stretching vibration mode [35]. The band around 2350 cm^{-1} is assigned to the carbon disulfide (CS2) [36]. The aromatic ring C–H bending vibrations give the peaks around 750 cm^{-1}[37].

Raman spectra of films are shown in Figure 6. The films exhibit the Raman hump-like feature around 367and 568 cm^{-1} and the hump profiles are almost symmetric. Hump profiles in these regions were formed by Zn-S vibrations. It could not be possible to determine the Raman vibrations of ZnS and indium doping in Raman spectrum at 100-1000 cm^{-1} range as the crystals forming the films were very small like 4-5 nm.

3.3. UV-visible studies of the films

The optical constants of thin films vary considerably with respect to the types of materials, the size and amount of nanoparticles therein. The determination of the optical constants of the semiconductors is one of the most important steps of producing materials fit for the purpose. The optical properties and performances of films can be calculated from the values of optical transmittance and reflectance spectra. For this purpose, optical transmittance and reflectance spectra of ZnS and ZnS:In films were measured at room temperature and shown in Figure 7 a and b. Optical transmittan-

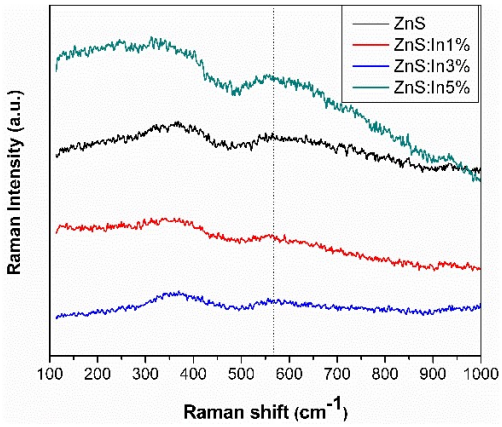

Fig. 6 - Raman spectra of the nanostructured ZnS and ZnS:In films.

ce spectra of the films changed by doping amount. Maximum transmittance of the films is around 80% at 700 nm and this shows that these films are suitable for photovoltaic applications. Indium doping changed transmittance values of ZnS films around 400-700 nm range. These transmittance changes are associated with increasing carrier concentration by In effect. Indium addition, rougher surfaces due to indium doping may decrease transmittance values of the films as rougher surfaces cause losses due to reflection and dispersion. This result is supported by increasing reflectance values of indium doped ZnS films in the visible region through indium doping. The steep optical transmittance shows homogeneous distribution of the particles and low defect density near the band edge. A slight blue shift was observed on the edge of the transmittance with increasing doping content in the films [24]. It was observed by increasing In doping rate that the reflectance values of ZnS:In3% and ZnS:In5% films were higher in the visible region while the reflectance values of these films were

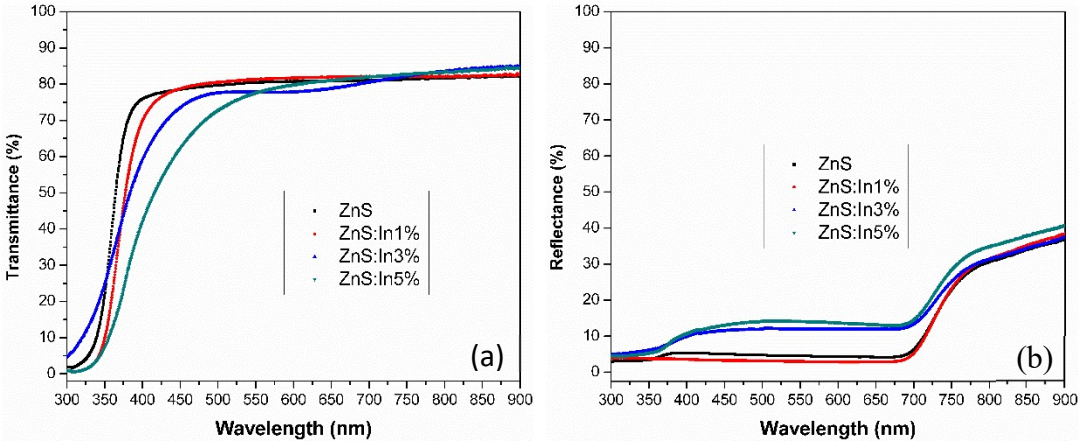

Fig. 7 - (a) The transmittance (b) reflectance spectra of nanostructured ZnS and ZnS:In films.

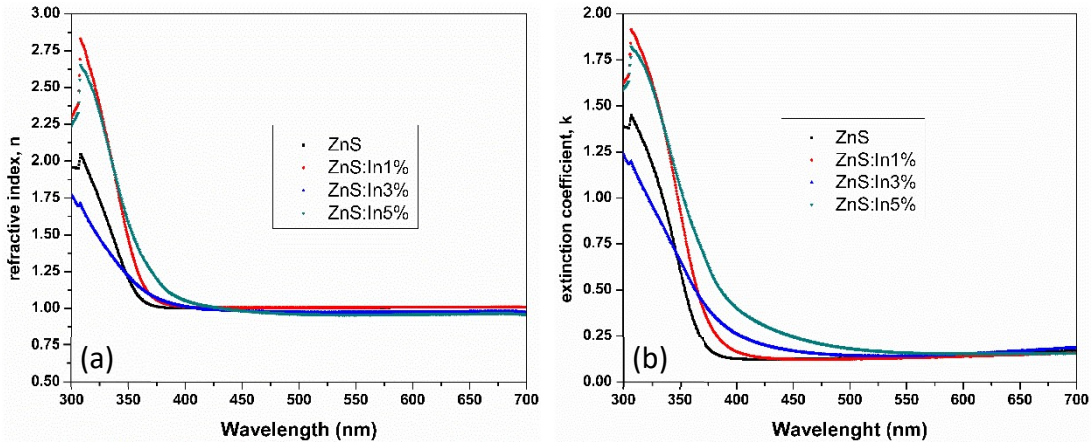

Fig.8 - Variation of (a) refractive index (b) extinction coefficient of the films with wavelength.

almost the same in other region. Roughness and various homogeneous structure of the surface of films and reflectance events from the surface and particle borders are the most important factors influencing measurements. Since the thicknesses of the films are about the same (about 300 nm order), the effect on the optical properties is not very high. Refractive index (n) and extinction coefficient (k) values of the films were calculated through absorbance and reflectance spectra and values based on wavelength are shown respectively in Figure 8a and 8b.

Refractive index of the films have been calculated by means of the following equation [38] ;

$$n = \left(\frac{1+R}{1-R}\right) - \sqrt{\frac{4R}{(1-R)^2} - k^2} \qquad (1)$$

In this equation, *k* is expressed as $k = \alpha\lambda/4\pi$ equation while R is the reflectance.

It is seen that both the refractive index and extinction coefficient values of the films decrease with the increase in the wavelength. The refractive index decreased with increasing wavelength and became fairly flat at higher wavelengths, showing normal dispersion behavior [30]. It is observed that the refractive index values of the films are 550 nm and at the same values for the longer wavelengths. Refractive index does not only influence the optic route of light, but also influences the amount reflected from a surface. If, refractive index of a solid increases, reflection increases, as well. Extinction coefficients of the films got values near-zero around 500-700 nm wavelength range and this result is consistent with the transmittance spectra results shown in Figure 7. The decrease in the extinction coefficient with an increase in wavelength shows that the fraction of light lost due to scattering and transmittance increases. Extinction coefficient of a material is based on its absorption values.

Optical band gaps of undoped and indium doped ZnS films were shown in Figure 9 (a). The optical band gap is evaluated according to the well-known Tauc's relation [39]: $\alpha E = A(E - E_g)^m$ (2)

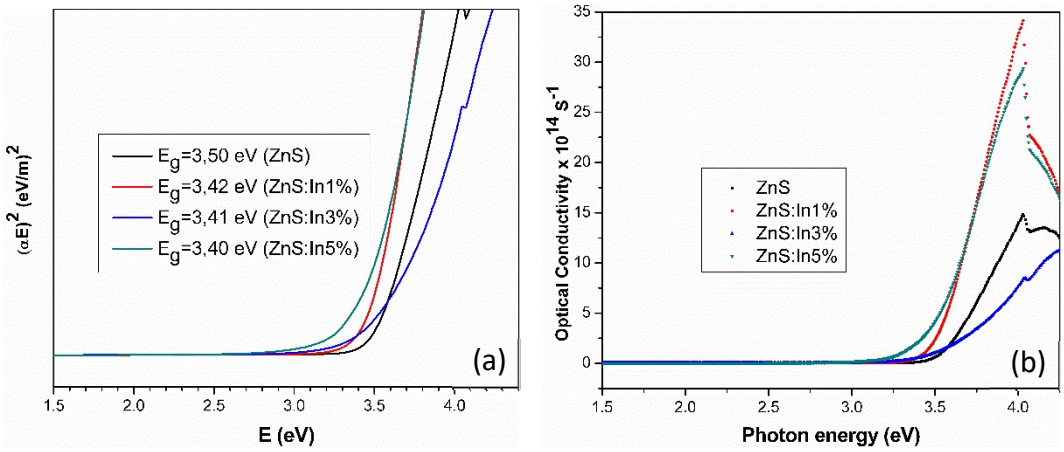

Fig. 9 - (a) The plots of (α E)^2 vs. E (b) Optical conductivity versus photon energy for the films.

where *A* is a constant, α is the absorption coefficient, *E* is the photon energy and E_g is the optical band gap. The band gap can be obtained by extrapolating the linear portion of the plot (α *E)*^{2} vs *E* to $\alpha = 0$.

Optical band gaps of the films decreased from 3.50 eV to 3.40 eV by increasing indium doping. The shrinking band width energy is based on the presence of In in ZnS structure, which causes the formation of new recombination centers through low emission energy (shrinkage effect) [40]. Carrier concentration increasing by In effect might have contributed Eg to drift towards a larger wavelength.

The optical response of the films was investigated optimally for optical conductivities. The following relation is used to calculate the optical conductivity of the film [41]:

$$\sigma = \left(\frac{\alpha nc}{4\pi} \right) \qquad (3)$$

where n is the the refractive index, α is the absorption coefficient and *c* is the velocity of light. Figure 8b shows the plot of optical conductivity versus photon energy. The optical conductivity is directly related with the absorption coefficient and refractive index of the material and is found to follow the same trend as that of the absorption coefficient (Fig 10) and the refractive index with increasing wavelength.

4. Conclusion

ZnS and ZnS:In films were produced my means of ultrasonic spray pyrolysis method by spraying on glass substrates heated up to 300±5 °C. The effect of In on the structural and optical characteristics of the ZnS films were analyzed. XRD spectra showed that indium doping decreased crystallinity. Crystallite sizes of the films were calculated in 4.61-4.63 range and this result was

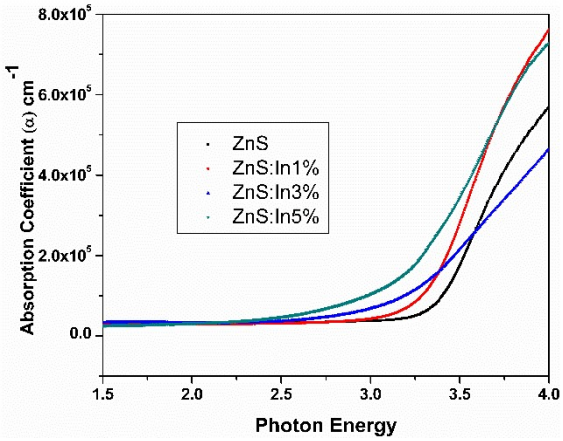

Fig. 10 - Absorption coefficient of the films.

confirmed by SEM analyses. The films exhibit the Raman hump-like feature around 367 and 568 cm^{-1} and the hump profiles are almost symmetric. Rougher surfaces due to indium doping decreased transmittance values of the films around 400-700 nm as rougher surfaces caused losses due to reflection and dispersion. Maximum transmittance of the films are around 80% at 700 nm. Optical conductivity values directly related with the absorption coefficient and refractive index of the material is calculated and is found to follow the same trend as that of the absorption coefficient and the refractive index with increasing wavelength.

Acknowledgement
Hereby, thanks Mrs. Vildan Bilgin for the stage of preparation of films, Mrs. Özge Bağlayan for the Raman and FTIR spectroscopy, Mrs. Seval Aksoy for UV-vis measurements.

REFERENCES

1. M. Tan, W. Cai, L.Zhang, Optical absortion of ZnS nanocrystals inside pores of silica. J. Appl. Phys. Lett., 1997, **71**, 3697.
2. W. Chen, Z. Wang, Z. Lin, L. Lin, Absorption and luminescence of the surface states in ZnS nanoparticles, J. Appl. Phys., 1997**, 82**, 3111.
3. P. Yang, M. Lii, Y. Dong, X. Duolong, G. Zhou, Photoluminescence properties of ZnS nanoparticles co-doped with Pb^{2+} and Cu^{2+}, J. Chem. Phys. Lett., 2001, **336**, 76.
4. B. Bhattacharjee, D. Ganguli, K. Iakoubovskii, A. Stesmans, S. Chaudhuri, Synthesis and characterization of sol gel derived ZnS: Mn^{2+} nanocrystallites embedded in a silica matrix, Bull Mater. Sci., 2002, **25,** 175.
5. R.P. Raffaelle, S.L. Castro, A.F. Hepp, S.G. Bailey, Quantum dot solar cells, Progress in Photovoltaics: Research and Applications, 2002, **10**, 433.
6. H. Metin, R. Esen, Annealing studies on CBD grown CdS thin films, J. Cryst. Growth, 2003, **258**, 141.
7. H. Moualkia, S. Hariech, M.S. Aida, Structural and optical properties of CdS thin films grown by chemical bath deposition, Thin Solid Films, 2009, **518,** 1259.
8. F. Liu, Y. Lai, J. Liu, B. Wang, S. Kuang, Z. Zhang, J. Li, Y. Liu, Characterization of chemical bath deposited CdS thin films at different deposition temperature, J. Alloys Comp., 2010, **493**, 305.
9. C. Charles Kittel, Introduction to Solid State Physics, Seventh ed, Wiley, Singapore, 2003.
10. A. Yamada, K. Matsubara, K. Sakurai, S. Ishizuka, H. Tampo, P. J. Fons, K. Iwata, S. Niki, Effect of band offset on the open circuit voltage of heterojunction $CuIn_{1-x}Ga_xSe_2$ solar cells, Appl. Phys. Lett., 2004, **85**, 5607.
11. Y.P. Venkata Subbaiah, P. Prathap, K.T. Ramakrishna Reddy, Structural, electrical and optical properties of ZnS films deposited by close-spaced evaporation, Applied Surface Science, 2006, **253**, 2409.
12. A. Goudarzi, G.M. Aval, R.Sahraei, H. Ahmadpoor, Ammonia-free chemical bath deposition of nanocrystalline ZnS thin film buffer layer for solar cells, Thin Solid Films, 2008, **516**, 4953.
13. L.X. Shao, K.H. Chang, H. L. Hwang, Zinc sulfide thin films deposited by RF reactive sputtering for photovoltaic applications. Appl Surf Sci., 2003, **212-213**, 305.
14. M.M. Islam, S. Ishizuka, A.Yamada, K.Sakurai, S.Niki, T.Sakurai, K.Akimoto, CIGS solar cell with MBE-grown ZnS buffer layer, Solar EnergyMaterials & SolarCells, 2009, **93**, 970.
15. Y.P. Venkata Subbaiah, P. Prathap, K.T. Ramakrishna Reddy, Structural, electrical and optical properties of ZnS films deposited by close-spaced evaporation, Applied Surface Science, 2006, **253**, 2409
16. D. H. Hwang, J. H. Ahn, K. N. Hui, K. S. Hui, Y. G. Son, Structural and optical properties of ZnS thin films deposited by RF magnetron sputtering, Nanoscale Research Letters 2012, **7**, 26.
17. P. Roy, J. R. Ota, S. K. Srivastava, Crystalline ZnS thin films by chemical bath deposition method and its characterization, Thin Solid Films, 2006, **515**, 1912.
18. R. Zhang, B. Wang, L. Wei, Influence of RF power on the structure of ZnS thin films grown by sulfurizing RF sputter deposited ZnO, Mat. Chemis. and Phys., 2008, **112**, 557.
19. M.C. Lopez, J.P. Espinos, F. Martın, D. Leinen, J.R. Ramos-Barrado, Growth of ZnS thin films obtainedby chemical spray pyrolysis, The influence of precursors: Journal of Crystal Growth, 2005; **285**, 66.
20. V.L. Gayou, B. Salazar-Hernandez, M.E. Constantino, E. Rosendo Andres, T. Dıaz ,R. Delgado Macuil, M. Rojas Lopez, Structural studies of ZnS thin films grown on GaAs by RF magnetron sputtering, Vacuum, 2010, **84**, 1191.
21. P.K. Ghosh, S. Jana, S. Nandy, K.K. Chattopadhyay, Size-dependent optical and dielectric properties of nanocrystalline ZnS thin films synthesized via rf-magnetron sputtering technique, Materials Research Bulletin, 2007, **42**, 505.
22. Z. Chen, X. X. Li, G. Duc, Q. Yu, Photoluminescence spectra of ZnS:X (X = F and I) nanoparticles synthesized via a solid-state reaction, Optical Materials, 2014, **36**, 1007.
23. R.N. Bhargava, D. Gallagher, Phys. Rev. Lett., Optical properties of manganese-doped nanocrystals of ZnS, 1994, **72**, 416.
24. K. Nagamani, P. Prathap, Y. Lingappa, R. W. Miles and K.T. R. Reddy, Properties of Al-doped ZnS Films Grown by Chemical Bath Deposition, Physics Procedia, 2012, **25**, 137.
25. N. Bitri, K. Ben Bacha, I. Ly, H. Bouzouita, M. Abaab, Studies of physical properties of the Al doped ZnS thin films prepared by Spray, J Mater Sci: Mater Electron, 2017, **28**, 734.
26. S.R. Chalana, R. Jolly Bose, R. Reshmi Krishnan, V.S. Kavitha, R. Sreeja Sreedharan, V.P. Mahadevan Pillai, Structural phase modification in Cu incorporated nanostructured zinc sulfide thin films, J. of Phys. and Chem. of Solids, 2016, **95**, 24.
27. D. Saikia, R.D. Raland, J.P.Borah, Influence of Fe doping on the structural, optical and magnetic properties of ZnS diluted magnetic semiconductor, Physica E, 2016, **83**, 56.
28. K. Nagamani, N. Revathi, P. Prathap, Y. Lingappa, K.T. Ramakrishna Reddy, Al-doped ZnS layers synthesized by solution growth method, Current Applied Physics, 2012, **12**, 380.
29. S. P. Patel, J.C. Pivin, A.K. Chawla, R. Chandra, D. Kanjilal, L. Kumar, Room temperature ferromagnetism in $Zn_{1-x}Co_xS$ thin films with wurtzite structure, Journal of Magnetism and Magnetic Materials, 2011, **323**, 2734.
30. A. Jrad, T. Ben Nasr, N. Turki-Kamoun, Study of structural, optical and photoluminescence properties of indium-doped zinc sulfide thin films for optoelectronic applications, Optical Materials, 2015, **50**, 128.
31. P. Babu, M. R. V. Reddy, S. Kondaiah, K. T. R. Reddy, P. Chinho, Chemical bath deposition of Mn-doped ZnS thin films using greener complexing agents: Effect of Mn-doping on the optical properties, Optik 2017, **130**, 608.
32. A. Jrad, T. B. Nasr, N. Turki-Kamoun, Study of structural, optical and photoluminescence properties of indium-doped zinc sulfide thin films for optoelectronic applications, Optical Materials 2015, **50**, 128.
33 T. Hurma, Structural and optical properties of nanocrystalline ZnS and ZnS:Al films, Journal of Molecular Structure, 2018, **1161**, 279.
34. Y. Infahsaeng, S. Ummartyotin, Investigation on structural properties of Al-substituted ZnS particle prepared from wet chemical synthetic route, Results in Physics, 2017, **7**,1245.
35. D. Amaranatha Reddy, C. Liu, R.P. Vijayalakshmi, B.K. Reddy, Effect of Al doping on the structural, optical and photoluminescence properties of ZnS nanoparticles, Journal of Alloys and Compounds, 2014, **582**, 257.
36. N. Shanmugam, S. Cholan, N. Kannadasan, K. Sathishkumar, G. Viruthagiri, Luminance behavior of Ce^{3+} doped ZnS nanostructures, Spectrochimica Acta Part A: Molecular and Biomolecular Spectroscopy, 2014, **118**, 557.
37. S. Sambasivama, B.K. Reddy, A. Divya, N. Madhusudhan Rao, C.K. Jayasankar, B. Sreedhar, Optical and ESR studies on Fe doped ZnS nanocrystals, Physics Letters A, 2009, **373**, 1465.
38. M. Caglar, Y. Caglar, S. Ilican, Investigation of the effect of Mg doping for improvements of optical and electrical properties, Physica B, 2016, **485**, 6.
39 J. I. Pankove, Optical process in semiconductors, Prentice Hall Inc., New York, 1971.
40. Y. Caglar, M. Caglar, S. Ilican, Microstructural, optical and electrical studies on sol gel derived ZnO and ZnO:Al films, Current Applied Physics, 2012, **12**, 963.
41. T. C. S. Girisun, S. Dhanuskodi, Linear and Nonlinear Optical Properties of Tristhiourea Zinc Sulphate (ZTS) Single, Cry. Resear. Tech., 2009, **44**, 1297.

****